Rate Enhancement and Retardation Strategies in Living Free Radical Polymerizations Mediated by Nitroxides and Other Persistent Species: A Theoretical Assessment

Marc Souaille and Hanns Fischer*

Physikalisch-Chemisches Institut der Universität Zürich, Winterthurerstrasse 190, CH 8057 Zürich, Switzerland

Received May 21, 2001; Revised Manuscript Received September 4, 2001

ABSTRACT: Three strategies to improve the performance of living and controlled polymerizations mediated by persistent radicals are analyzed kinetically to explore their advantages and limits. First, rate enhancements by an additional conventional initiation or by the monomer self-initiation are found only compatible with high degrees of polymer livingness and control if the additional initiation rate is much smaller than the activation rate of the dormant polymer. Second, rate-enhancing reductions of the persistent radical concentration by reactions with additives or by a natural decay lead to living and controlled polymers even if these processes are surprisingly fast. The enhanced monomer conversion rates generally diminish the detrimental effects of a direct precursor decay or of the radical disproportionation to unreactive products. Third, a retarding initial excess of the persistent species can force unfavorably fast systems to livingness and control. The limits of these procedures are specified. Analytic equations are given which facilitate the extraction of kinetic data from conversions, degrees of polymerization and polydispersities. They agree with experimental findings.

Introduction

Living and controlled free radical polymerizations mediated by nitroxides and other persistent radicals[1−3] yield polymers with small polydispersities, controlled molecular weights, and reactive end groups that allow chain extensions and block copolymer formation. The minimal mechanism involves the reversible cleavage (eqs 1 and 2) of dormant polymer chains R_n−Y with n monomer units into persistent radicals Y$^\bullet$ and transient carbon-centered radicals $R_n^\bullet$ and the usual radical propagation (eq 3) and termination (eq 4) steps. It is often initiated by low molecular weight compounds R_0−Y.[3]

$$R_n\text{−Y} \rightarrow R_n^\bullet + Y^\bullet \quad (1)$$

$$R_n^\bullet + Y^\bullet \rightarrow R_n\text{−Y} \quad (2)$$

$$R_n^\bullet + M \rightarrow R_{n+1}^\bullet \quad (3)$$

$$R_n^\bullet + R_m^\bullet \rightarrow P_n + P_m \quad (4)$$

During the polymerizations the self-termination of the propagating radical (eq 4) causes a build-up of an excess of the persistent species. Thereby, the cross-coupling (eq 2) is accelerated, and the self-termination (eq 4) is retarded although it never stops completely. If the monomer is consumed before appreciable self-termination (eq 4) has occurred, the desired dormant polymer chains R_n−Y are the major products.

In other fields of chemistry, the dominance of radical cross-couplings in systems involving transient and persistent radicals is long known, and the phenomenon is called the persistent radical effect (PRE).[4] For living polymerizations, the preferred cross-coupling was first utilized by Otsu.[5] Later, Solomon et al., Georges et al., Wayland et al., Matyjaszewski et al., Percec et al., Fukuda et al., and other authors[1−3,6] provided convincing examples and additional independent mechanistic insight. Living atom transfer radical polymerizations (ATRP) follow the same principle.[3]

In earlier theoretical work[7] we have analyzed the kinetics and the chain length distribution of living polymerizations following (1) to (4) in the absence of any additional reaction and for the initial presence of only a low molecular weight initiating compound R_0−Y and the monomer M. The equations for the radical concentrations for this basic case were also derived by Fukuda et al.[8] In addition, we have analyzed the detrimental effects of direct decompositions of the dormant chains and of the disproportionation between Y$^\bullet$ and $R_n^\bullet$ to unreactive products.[9]

Such living polymerizations are characterized by a quasi-equilibrium of the reversible decay (eqs 1 and 2) with weakly time-dependent radical concentrations, by a considerable excess of the persistent radical and by an extremely prolonged lifetime of the dormant species. They require that the rate constants of the reactions 1 and 2 fulfill conditions which depend on the self-termination constant and on the initial precursor concentration. Moreover, large conversions, low polydispersities, and small fractions of unreactive polymer are only obtained in reasonable times if these rate constants obey further conditions which depend on the propagation constant and the initial monomer concentration.[7]

The permanently growing excess of the persistent species retards the polymerization and leads to long polymerization times if the rate constants of reactions 1 and 2 are not within the proper ranges.[7] To overcome this difficulty, Matyjaszewski[10] and Fukuda[11] introduced the addition of a slowly decomposing conventional initiator. This enhances the conversion rate but it must

* Corresponding author. Fax: 0041 1 635 68 56. E-mail: hfischer@pci.unizh.ch.

10.1021/ma010880h CCC: $22.00
Published on Web 11/30/2001

not necessarily deteriorate the livingness and the control as long as the additional initiation governs the rate, while the equilibrium holds and remains responsible for the control.[10−13] Related to this external initiation is the acceleration of the conversion by the monomer auto-initiation in regulations employing nitroxides which provide unfavorable rate contants, as for styrene using 2,2,6,6-tetramethylpiperidine-*N*-oxyl (TEMPO).

The conversion times are also shortened by a built-in instability of the persistent radicals that leads to additional transient radicals.[14] The partial removal of persistent radicals by reactions with additives[15] has the same effect and may often also lead to additional transient species.

A further problem arises from the fact that a good control of the molecular weight and a low polydispersity index require that the decay (activation) of the regulator R_0−Y in reaction 1 is fast compared to the monomer conversion because all chains should start to grow nearly instantaneously. This is difficult to achieve for rapidly propagating monomers. The counter-strategy is to add a small amount of persistent species before the reaction.[16] It slows down the conversion but improves the control, and it also prevents exothermicity effects. In this case, the equilibrium between reactions 1 and 2 is initially determined by the excess concentration, and this allows the extraction of kinetic data from polymerization rates.[16−19]

The rate enhancements necessarily lead to less controlled polymerizations and the initial excess of the persistent species necessarily prolongs the time needed for conversion. Here, we analyze these strategies theoretically and explore the limits to which they can be extended without causing large detrimental effects. We also discuss specific experimental examples mainly from nitroxide-mediated systems, but the main conclusions and the rate laws are valid for all living radical polymerizations involving persistent controlling species, including ATRP. Further, we show that the external rate enhancements beneficially diminish the effects of reactions which bring living radical polymerizations to a premature end.[9]

Rate Enhancement by Additional External Radical Generation

Radical Concentrations and Polymerization Rates. In this and in the following sections, we assume chain-length independent rate constants. This allows us to consider only the sums of the concentrations [R] of all propagating radicals $R_n^\bullet$, [I] of all dormant species R_n−Y, [P] of all unreactive polymer products P_n besides the concentration [Y] of the persistent radical $Y^\bullet$.[7,9] We also consider self-termination of the propagating radicals by disproportionation only (eq 4). Termination by combination would halve the concentration and double the degree of polymerization of the small unreactive polymer fraction, but it does not affect the kinetics. The rate constants of reactions 1−4 are denoted by k_d (1), k_c (2), k_p (3), and k_t (4), respectively.[20] If these reactions occur exclusively, the existence of the quasi-equilibrium for reactions 1 and 2 and the desired dominance of the cross-coupling require that the rate constants of the reversible cleavage obey the conditions

$$K = k_d/k_c \ll k_c[I]_0/k_t, \quad K \ll [I]_0, \quad \text{and} \quad k_d \le k_t[I]_0, \tag{5}$$

and the first condition is usually the strongest.[7,9] $K = k_d/k_c$ is the equilibrium constant, and $[I]_0$ is the initial concentration of the dormant species. These conditions shall be also fulfilled in the presence of the additional reactions.

We first cover the effects of an external or a monomer self-initiation with a constant rate R_i, that is, we consider the reaction

$$\text{radical source} \xrightarrow{R_i} R_0^\bullet \tag{6}$$

in addition to reactions 1−4. Reaction 6 enhances the conversion rate, and the formation of self-termination products, and we search for the upper limit of R_i which still provides sufficient livingness and control.

In the absence of excess persistent species, the initial concentrations are

$$[I](t=0) = [I]_0 \neq 0, \quad \text{and} \quad [Y]_0 = [R]_0 = [P]_0 = 0 \tag{7}$$

and at later times the concentrations obey the stoichiometry

$$[I]_0 - [I] = [Y] = [R] + [P] - R_i t \tag{8}$$

Since [I] and [P] can be calculated if [R] and [Y] are known, it is sufficient to solve the kinetic equations for the radical concentrations [R] and [Y][20]

$$\frac{d[R]}{dt} = k_d([I]_0 - [Y]) - k_c[R][Y] - k_t[R]^2 + R_i \tag{9a}$$

$$\frac{d[Y]}{dt} = k_d([I]_0 - [Y]) - k_c[R][Y] \tag{9b}$$

A solution of these equations has first been found by Fukuda et al.[12,13] These authors used the relation $d[R]/dt \ll d[Y]/dt$ and preassumed the equilibrium

$$k_c[R][Y] = k_d[I]_0 \tag{10}$$

This is valid if the conditions in (5) are obeyed.[7] Subtraction of (9a) from (9b), neglect of $d[R]/dt$, and replacement of [R] by [Y] using (10) gives an equation which after the separation of variables is integrated via partial fractions to

$$\ln\frac{1+x}{1-x} - 2x = 2\left(\frac{R_i^3}{k_t K^2 [I]_0^2}\right)^{1/2} t, \tag{11}$$

where $x = (R_i/k_t)^{1/2}[Y]/K[I]_0$.[12,13] This equation is implicit in [Y]. For sufficiently small x and combined with (10) it leads to the radical concentrations

$$[R] = (K[I]_0/3k_t)^{1/3} t^{-1/3} \quad \text{and} \quad [Y] = (3k_t K^2 [I]_0^2)^{1/3} t^{1/3} \tag{12}$$

and these are the solutions known for for $R_i = 0$.[7,8] For $x \to 1$, eq 11 yields the stationary radical concentrations

$$[R]_s = \left(\frac{R_i}{k_t}\right)^{1/2} \quad \text{and} \quad [Y]_s = K[I]_0\left(\frac{k_t}{R_i}\right)^{1/2} \tag{13}$$

In this stationary state, the transient radical concentration is governed by the additional radical generation rate R_i and by the termination constant as in a

conventional polymerization, whereas the concentration of the persistent species is governed by $[R]_s$ and the equilibrium (10). The constant $[R]_s$ leads to a linear time dependence of the polymerization index as for a conventional radical polymerization.

$$\ln\frac{[M]_0}{[M]} = k_p\left(\frac{R_i}{k_t}\right)^{1/2} t \tag{14}$$

To derive these equations without preassumptions and to find the conditions for their validity we apply a phase space analysis of the kinetic equations, as before.[7,9] It is convenient to introduce a set of reduced quantities that underline the kinetically relevant ratios

$$a = \frac{k_c[I]_0}{k_d}, \quad b = \frac{k_t[I]_0}{k_d}, \quad r = \frac{R_i}{k_d[I]_0} \tag{15a}$$

$$\rho = \frac{[R]}{[I]_0}, \quad \eta = \frac{[Y]}{[I]_0}, \quad \tau = k_d t \tag{15b}$$

With the further notation $\dot{x} = dx/d\tau$, the kinetic eq 9 then becomes

$$\dot{\rho} = 1 - \eta - a\rho\eta - b\rho^2 + r \tag{16a}$$

$$\dot{\eta} = 1 - \eta - a\rho\eta \tag{16b}$$

In this notation, the conditions in (5) for the existence of the quasi-equilibrium (10) and for the dominance of the cross-coupling in the absence of the additional radical generation read $a^2 \gg b$, $a \gg 1$, and $b = 1$, or in short $a^2 \gg b = 1$.

Next, we consider the general behavior of the trajectory of the point $(\rho(\tau), \eta(\tau))$ in the phase space spanned by the variables ρ and η and of their zero isoclines. These are defined by zero time derivatives in eq 16, that is by

$$\eta_1 = \frac{1 + r - b\rho^2}{1 + a\rho} \quad \text{and} \quad \eta_2 = \frac{1}{1 + a\rho} \tag{17}$$

respectively, and they cross at

$$\rho_s = \left(\frac{r}{b}\right)^{1/2} \quad \text{and} \quad \eta_s = \frac{1}{1 + a\left(\frac{r}{b}\right)^{1/2}}, \tag{18a}$$

or

$$[R]_s = \left(\frac{R_i}{k_t}\right)^{1/2} \quad \text{and} \quad [Y]_s = \frac{[I]_0}{1 + \frac{1}{K}\left(\frac{R_i}{k_t}\right)^{1/2}} \tag{18b}$$

The crossing point is a stable focus that is reached for any initial condition, that is, the stationary state. Equation 18 does not provide equilibrium 10 directly, and the equation for $[Y]_s$ is not identical to Fukuda's result (eq 13). However, eqs 10 and 13 follow from eq 18 if the parameters obey $a\sqrt{r/b} \gg 1$, that is, if $[R]_s = \sqrt{R_i/k_t} \gg K$, or $a^2/b \gg 1/r$. Since $a^2/b \gg 1$ will hold anyway, the new condition $a^2/b \gg 1/r$ does not provide an upper limit for the additional initiation rate. However, for living polymerizations without the additional initiation, the rate of the cross- reaction must also dominate over the rate of the self-termination (4),[7] that is

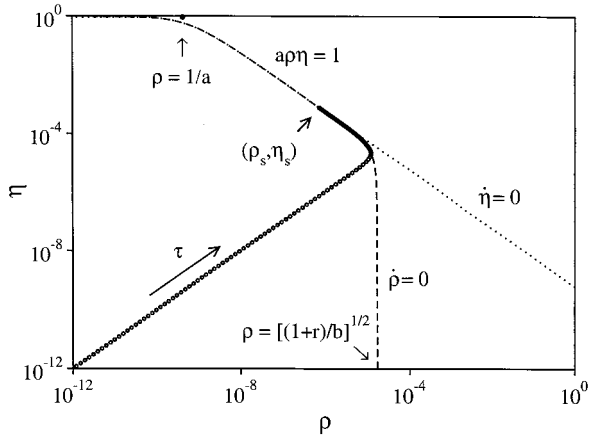

Figure 1. Time evolution of the reduced concentrations ρ and η of the radicals R• and Y• and of the isoclines in the phase space for a small relative rate of additional initiation. Parameters: $a = 1.67 \times 10^9$, $b = 3.33 \times 10^9$, and $r = 0.002$ ($k_d = 3 \times 10^{-3}$ s^{-1}, $k_c = 5 \times 10^7$ M^{-1} s^{-1}, $k_t = 10^8$ M^{-1} s^{-1}, $[I]_0 = 0.1$ M, $R_i = 6 \times 10^{-7}$ M s^{-1}).

$$k_c[R][Y] \gg k_t[R]^2 \tag{19}$$

This condition and eq 18b provide

$$r \ll 1 \quad \text{or} \quad R_i \ll k_d[I]_0 \tag{20}$$

Obviously, a large dominance of the cross-coupling in the stationary state requires that the rate R_i of the additional external radical generation is very small compared to the rate $k_d[I]_0$ of the internal radical generation by the cleavage (activation) of the dormant species.

Figure 1 shows a trajectory calculated for experimentally reasonable parameters $a = 1.67 \times 10^9$, $b = 3.33 \times 10^9$, and $r = 0.002$ ($k_d = 3 \times 10^{-3}$ s^{-1}, $k_c = 5 \times 10^7$ M^{-1} s^{-1}, $k_t = 10^8$ M^{-1} s^{-1}, $[I]_0 = 0.1$ M, $R_i = 6 \times 10^{-7}$ M s^{-1}) together with the isoclines (eq 17). For the chosen small r, the trajectory first evolves as for $r = 0$.[7] It follows the line $\rho = \eta = \tau$, and then it crosses the isocline η_1 and remains confined to the region between the two isoclines thereafter.[7,9] However, instead of approaching $\rho = 0$ and $\eta = 1$ as for $R_i = 0$,[7] it ends at the stationary state (eq 13), and ρ remains larger and η smaller than the final values reached without the additional radical generation.

Before reaching the stationary point, both zero isoclines coincide on the line $a\rho\eta = 1$. This characterizes the quasi-equilibrium regime with the weakly time-dependent radical concentrations (eq 12).[7] Hence, for small r the radical concentrations first follow $[R] = [Y] = k_d[I]_0 t$, then eq 12, and finally eq 13, and the complete set of conditions for this behavior is $a^2 \gg b \geq 1 \gg r$ or $R_i \ll k_d[I]_0 \leq k_t[I]_0 2 \ll k_c 2[I]_0 3/k_d$.

By setting the different relations for the persistent radical concentration in the different time regimes equal to one another, one obtains the times for the transition from the initial to the intermediate t_1 and from the intermediate to the stationary state regimes t_2 as

$$t_1 = \left(\frac{3k_t}{k_d k_c^2 [I]_0}\right)^{1/2} \quad \text{and} \quad t_2 = \frac{K[I]_0}{3R_i}\left(\frac{k_t}{R_i}\right)^{1/2} \tag{21}$$

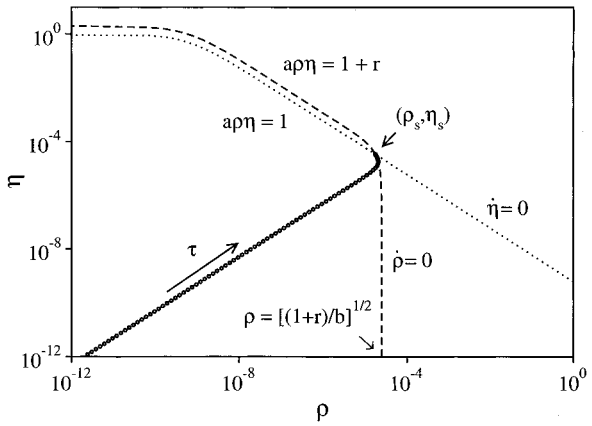

Figure 2. Time evolution of the reduced concentrations ρ and η of the radicals R$^\bullet$ and Y$^\bullet$ and of the isoclines in the phase space for a large relative rate of additional initiation. Parameters as for Figure 1 but $r = 1$ ($R_i = 3 \times 10^{-4}$ M s^{-1}).

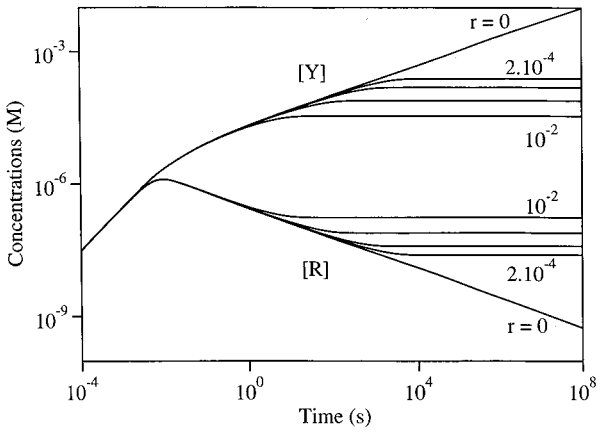

Figure 3. Numerically computed time evolutions of the radical concentrations [R] and [Y] for different relative rates of additional initiation $r = R_i/k_d[I]_0 = 0$, 2×10^{-4}, 5×10^{-4}, 2×10^{-3}, and 10^{-2}. Other parameters are as for Figure 1. The log−log plot serves to enhance the visibility of the different time regimes.

These expressions are approximate because the transitions are not sharp. The intermediate solutions (eq 12) exist if $t_1 \ll t_2$. This yields $R_i \ll k_d[I]_0/3$ or $r \ll 1/3$, a relation that is practically equal to the condition $r \ll 1$ found above. For the parameters of Figure 1, the intermediate regime (eq 12) lasts from about 0.02 s to about 6 min. Then the stationary state is reached. The trajectory of Figure 2 holds for the same parameters as used for Figure 1 except for a larger $r = 1$, that is, $R_i = k_d[I]_0 = 3 \times 10^{-4}$ M s^{-1}. Now, the stationary state is reached very fast in $t_2 = 30$ ms. In the stationary state, the zero isocline η_2 is still approximated by $\eta_2 = 1/a\rho$, which means that the equilibrium condition 10 is fulfilled. However, the rate of the cross-reaction is no longer much larger than the self-termination rate of the transient radicals. Hence, for the large r there will be little living radical polymerization. This example shows that the existence of the equilibrium alone does not suffice for a living process. Figure 3 shows a log−log plot of numerically calculated radical concentrations against the time for the parameters used for Figure 1 but for various values of r. Such a log−log plot enhances the distinction between the different time regimes. With increasing relative rate r the additional radical generation locks [R] to larger and [Y] to smaller stationary values.

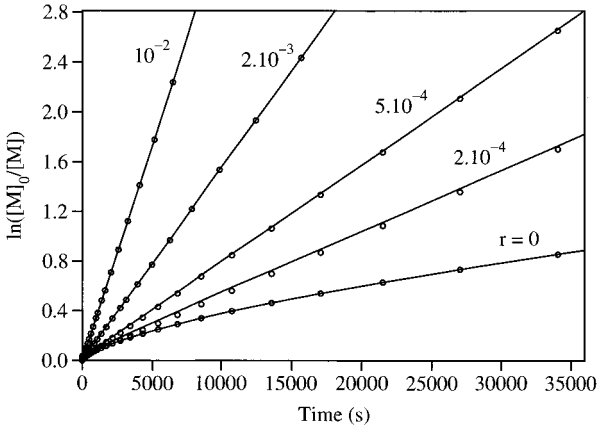

Figure 4. ln([M]$_0$/[M]) vs time for different relative rates of additional initiation $r = R_i/k_d[I]_0$. Solid lines are from numerical calculations, and circles are according to eqs 23 and 24. Other parameters are as for Figure 1, $k_p = 2000$ M^{-1} s^{-1}, and $[M]_0 = 10$ M.

The rate equation for the monomer consumption

$$\frac{d[M]}{dt} = -k_p[R][M] \tag{22}$$

is easily integrated using the expressions for [R] (12, 13). If, as usual, $k_p \ll 3\,k_c$, one can neglect the monomer conversion in the very short initial period of equal [R] and [Y].[7] Hence, for small r one reobtains the result for $R_i = 0$.[7]

$$\ln\frac{[M]_0}{[M]} = \frac{3}{2}k_p\left(\frac{K[I]_0}{3k_t}\right)^{1/3} t^{2/3} \tag{23}$$

This equation is valid up to the transition to the stationary state at the approximate time t_2, and thereafter one has

$$\ln\frac{[M]_0}{[M]} = \frac{k_p k_d[I]_0}{2k_c R_i} + k_p\left(\frac{R_i}{k_t}\right)^{1/2}(t - t_2) \tag{24}$$

The first term on the right-hand side is very small compared to one if $R_i \gg k_p k_d[I]_0/2k_c$. Then the monomer conversion occurs essentially only in the stationary state. For $k_p = 2000$ M^{-1} s^{-1} and $k_c = 5 \times 10^7$ M^{-1} s^{-1}, this requires a minimum relative rate $r \gg 2 \times 10^{-5}$ or $R_i \gg 0.00002k_d[I]_0$. On the other hand, the additional initiation has practically no effect if the transition time t_2 (eq 21) is larger than the time needed for 90% monomer conversion. Using (23), this yields $R_i \leq k_p k_d[I]_0/2[\log(10)k_c]$ or $R_i \leq 0.00001k_d[I]_0$ and $r \leq 10^{-5}$. Obviously, for the parameters chosen above, already rather small additional initiation rates provide the stationary behavior of the radical concentrations. Of course, for larger values of k_p and for smaller values of k_c, the change of the rate law requires larger relative rates r. Figure 4 displays the time dependence of the conversion index ln[M]$_0$/[M] for the parameters given above and $k_p = 2000$ M^{-1} s^{-1} and $[M]_0 = 10$ M. The data were obtained by numerical integrations of the kinetic equations and from the analytical solutions (23) for $r = 0$ and (24) for $r \neq 0$. In the latter case, the polymerization index hardly shows the initial curvature which comes from the intermediate time regime. In actual polymerizations, some additional initiation may always be caused by minor radical generating impurities, as

peroxides or other thermally labile compounds. Therefore, the curved behavior of the polymerization index in the absence of deliberate additional initiation is difficult to observe if k_p is small and k_c is large and if the rate of internal radical generation $k_d[I]_0$ is small. Nevertheless, experimental examples for the $t^{2/3}$-dependence of $\ln[M]_0/[M]$ (eq 23) have been given for cases with sufficiently small ratio r both in nitroxide-mediated polymerizations and in ATRP.[8,21−23]

According to eq 23 and for the parameters chosen for Figure 4, one obtains 90% monomer conversion in 41.3 h if $r = 0$. An additional initiation with $r = 2 \times 10^{-3}$ reduces this time to 4.1 h, that is by a factor of 10. The substantial rate enhancement is due to the monomer conversion in the stationary regime where [R] keeps a reasonably high level. More generally, the ratio of the times for 90% conversion with and without additional initiation is calculated from eqs 23 and 24 as

$$\frac{t_{90}(r > 0)}{t_{90}(r = 0)} = \frac{3}{2^{3/2}(\log 10)^{1/2}}\left(\frac{k_p k_d [I]_0}{k_c R_i}\right)^{1/2} \qquad (25)$$

For $R_i > k_p k_d [I]_0/2k_c$ there will always be a considerable reduction of the conversion time.

Of course, the favorable rate enhancement is accompanied by an increase of the self-termination products. This is easily assessed. In the stationary state one has $[R]_s = \sqrt{R_i/k_t} \gg K$, $[Y]_s = K[I]_0/[R]_s \ll [I]_0$ from (18) and $[Y]_s \gg [R]_s$ from (19). The concentration of the unreactive polymer products P then follows by stoichiometry (eq 8) as

$$[P] = [Y]_s + R_i t \qquad (26)$$

Here, the term $[Y]_s$ reflects the transient radicals that stem from the dormant chains and have self-terminated, and $R_i t$ comes from the additionally generated radicals. Combination of eqs 26, 12, 13, 23, and 24 yields the ratio of unreactive products at 90% conversion with and without additional radical generation

$$\frac{[P]_{90}(r > 0)}{[P]_{90}(r = 0)} = \left(\frac{\log (10)}{2}\right)^{1/2}\left(\frac{k_c R_i}{k_p k_d [I]_0}\right)^{1/2}\left(1 + \frac{k_p k_d [I]_0}{k_c R_i \log(10)}\right) \qquad (27)$$

If eqs 13 and 24 hold, that is if $R_i \gg k_p k_d [I]_0/2k_c$, the second term in the last bracket in (27) is small compared to 1. Then, eqs 25 and 27 yield the simple result

$$\frac{[P]_{90}(r > 0)}{[P]_{90}(r = 0)} = 0.75\frac{t_{90}(r = 0)}{t_{90}(r > 0)} \qquad (28)$$

Thus, a time reduction by a given factor translates to 75% into the fractional increase of the self-termination products at large conversion. We show below that this need not largely reduce the quality of the resulting polymer if the fraction of unreactive products is anyway small in the absence of the additional radical generation.

Degree of Polymerization, Polydispersity, and Livingness. As before,[7] we calculate the time dependencies of the number average degree of polymerization $X_n = m_1/m_0$ and of the polydispersity index PDI = $m_0 m_2/m_1^2$ from the moments[24]

$$m_k = \sum_{n=1}^{\infty} n^k([I_n] + [R_n] + [P_n]) \quad k = 0, 1, 2$$

The exclusion of $n = 0$ in the summations ensures that only monomer-containing species are counted. It is necessary because we start from monomer free sources of $R_0^\bullet$. For high enough monomer concentrations, each radical $R_0^\bullet$ that is released from R_0−Y or formed by the additional initiation undergoes at least one addition before recoupling with $Y^\bullet$.[7,9] This leads to the zeroth moment, that is the chain concentration

$$m_0 = [I]_0(1 - e^{-k_d t}) + R_i t \qquad (29)$$

The total moments m_1 and m_2 obey the differential equations

$$\frac{dm_1}{dt} = -\frac{d[M]}{dt}, \qquad (30a)$$

$$\frac{dm_2}{dt} = -\frac{d[M]}{dt} + 2k_p[M]m_1(R) \qquad (30b)$$

and similar expressions hold for individual moments of $R^\bullet$, I, and P.[7] Integration of eq 30a and eq 29 yield

$$X_n = \frac{m_1}{m_0} = \frac{[M]_0 - [M]}{[I]_0(1 - e^{-k_d t}) + R_i t} \qquad (31)$$

The exponential term comes from the decay time $(k_d)^{-1}$ of R_0−Y.

Using conversion instead of time in (31) provides Figure 5. The data were calculated for the same parameters as used in Figures 1, 3, and 4. For $R_i = r = 0$, the number average degree of polymerization X_n increases linearly with the fractional monomer conversion C as $X_n = ([M]_0/[I]_0)C$ apart from the initial decrease that is caused by the time required to convert R_0−Y into monomer containing chains R_n−Y. This demonstrates a controlled process.

For $r \neq 0$ and at large conversions, X_n deviates negatively from the straight line, and the deviations increase with increasing relative rate r. This is caused by the creation of the additional chains. In particular, an additional initiation with $r = 2 \times 10^{-3}$, or $R_i = 6 \times 10^{-7}$ M s^{-1}, provides 90% conversion in about 4.1 h as opposed to 41 h for $r = 0$. It creates about 10^{-2} M additional chains in comparison to 10^{-1} M chains originating from R_0−Y. Hence, at large conversions X_n becomes about 10% smaller than the ideal value.

For low conversions the deviations from the curve for $R_i = r = 0$ increase also with increasing r, but they are positive. This is not due to the additional chain formation because this decreases X_n. It is explained by the fact that the additional initiation accelerates the conversion. Hence, as r increases the initial deviations caused up to the time $(k_d)^{-1}$ by the consumption of the regulator R_0−Y now extend to larger conversions.

Following the lines of ref 7b, an expression for the total polydispersity index PDI is derived. For sufficiently small monomer contents of the transient radicals and of the self-termination products, the kinetic equations of the individual moments provide the equation[7b]

$$\dot{m}_2 = -[\dot{M}] - 2[\dot{M}]([M]_0 - [M])/[I]_0 + 2k_p{}^2[M]^2[R]^2/k_d[I]_0 \qquad (32)$$

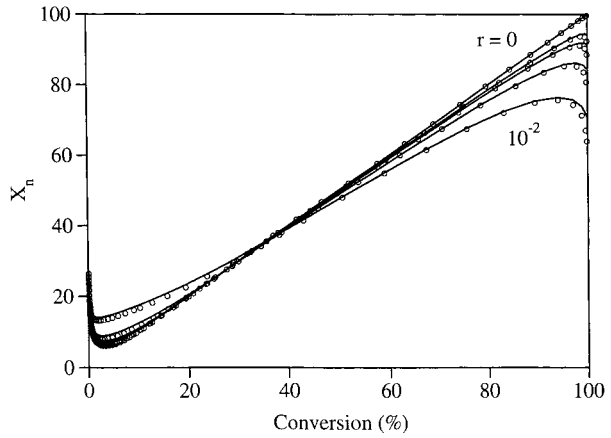

Figure 5. Number average degrees of polymerization as function of conversion for different relative rates of additional initiation $r = R_i/k_d[I]_0 = 0$, 2×10^{-4}, 5×10^{-4}, 2×10^{-3}, and 10^{-2}. Solid lines from numerical calculations and circles according to eq 31. Parameters are as for Figures 1, 3, and 4.

For sufficiently large r, eqs 13 and 14 hold, and then (32) integrates to

$$m_2 = ([M]_0 - [M])\left\{1 + ([M]_0 - [M])/[I]_0 + \frac{k_p}{k_d[I]_0}\left(\frac{R_i}{k_t}\right)^{1/2}([M]_0 + [M])\right\} \quad (33)$$

With the definition of the PDI, $m_1 = [M]_0 - [M] = [M]_0(1 - C)$ where C is the fractional monomer conversion and with eqs 29 and 31, one obtains from (33)

$$\mathrm{PDI} = (1 - e^{-k_d t} + R_I t/[I]_0)\left(1 + \frac{k_p}{k_d}\left(\frac{R_i}{k_t}\right)^{1/2}\frac{2 - C}{C}\right) + \frac{1}{X_n} \quad (34)$$

If $k_d t \gg 1$ and $R_i t \ll [I]_0$ at the observation time, this expression reduces to

$$\mathrm{PDI} = 1 + \frac{1}{X_n} + \frac{k_p}{k_d}\left(\frac{R_i}{k_t}\right)^{1/2}\frac{2 - C}{C} \quad (35)$$

and for small conversions $C \approx k_p(R_i/k_t)^{1/2}t \ll 1$ to

$$\mathrm{PDI}_0 = 1 + \frac{1}{X_n} + \frac{2}{k_d t} \quad (36)$$

In the absence of the additional radical generation the corresponding expression is[7]

$$\mathrm{PDI}_0 = 1 + \frac{1}{X_N} + \frac{8}{3k_d t}, \quad (37)$$

and the different numerical factors in (36) and (37) are due to the different time dependencies in (13) and (12) of the transient radical concentration.

Figure 6 shows polydispersity indices as functions of the time for two sets of r and k_d. The solid lines were calculated by numerical integrations of the moment equations,[7b] the squares with eq 34 and the circles with eq 36. For the smaller r, the analytical equations agree reasonably well with the more exact numerical solution in the whole time range. For the larger $r = 0.005$, there are large deviations, and the polydispersity increases at long times. However, the long times mean rather

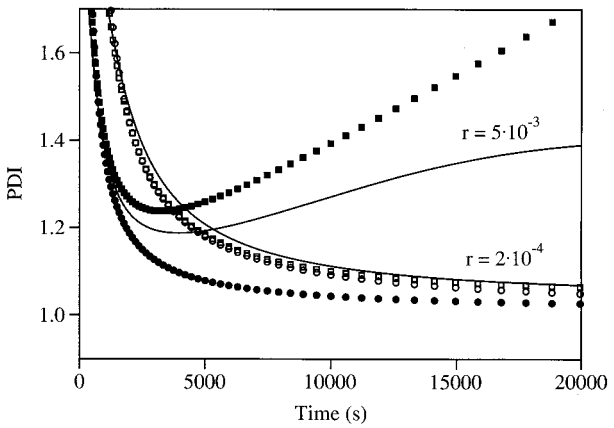

Figure 6. Polydispersity indices as function of time for two different relative rates of additional initiation $r = R_i/k_d[I]_0$ and different rate constants k_d. Straight lines are according to numerical integrations, squares are according to eq 34, and circles are according to eq 36. Key: open symbols, $r = 0.0002$, $k_d = 0.003\ s^{-1}$; closed symbols, $r = 0.005$, $k_d = 0.006\ s^{-1}$. Other parameters are as used for Figures 1, 3, and 4.

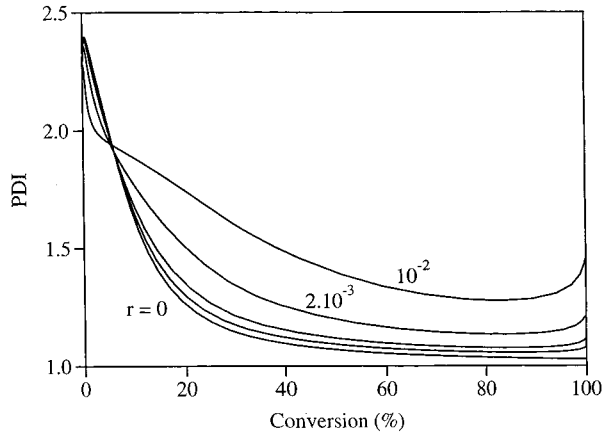

Figure 7. Polydispersity indices as function of conversion for different relative rates of additional initiation $r = R_i/k_d[I]_0 = 0$, 2×10^{-4}, 5×10^{-4}, 2×10^{-3}, and 10^{-2} according to numerical integrations Other parameters are as used for Figures 1, 3, and 4.

large conversions. Actually, plots of the numerically calculated polydispersities against the monomer conversion (Figure 7) show noticeable effects of the additional initiation, but they remain moderate as long as $r < 10^{-2}$.

Using a purely probabilistic approach involving a constant concentration of the growing chains and an equilibrium which strongly favors the dormant species, Fukuda et al. have derived eq 36 before.[11] It was applied to extract the rate constant k_d of reaction 1 from the time dependence of polydispersity indices observed during the polymerization of styrene starting from a polystyrene−TEMPO macroinitiator in the presence of additional initiation.[11,25] Then eq 36 holds even at times which are short compared to $(k_d)^{-1}$ because the exponential term in eqs 29, 31, and 34 comes from the exclusion of monomer free species and must be dropped if a monomer containing macroinitiator is used. In this respect we also notice that the stationary state (eq 13) is reached in times t_2 (eq 21) which are often much shorter than $(k_d)^{-1}$.

Further, the loss of livingness of the resulting polymer caused by the additional radical generation can be judged from the monomer fraction incorporated in the

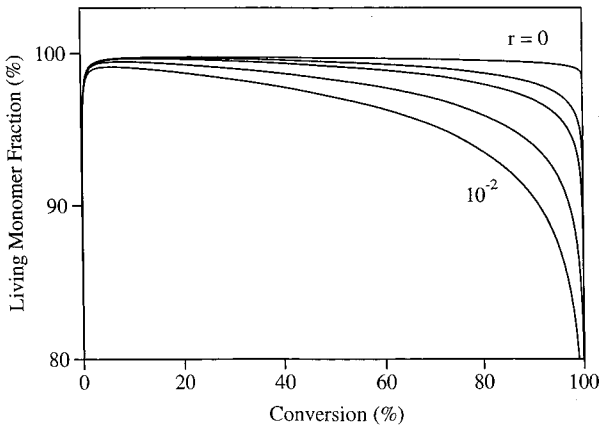

Figure 8. Numerically calculated monomer fractions in living polymer chains as function of conversion for different relative rates of additional initiation $r = R_i/k_d[I]_0 = 0$, 2×10^{-4}, 5×10^{-4}, 2×10^{-3}, and 10^{-2}. Other parameters are as for Figures 1, 3, and 4.

dormant chains R_n−Y. Numerical solutions of the equations for the first moments provide Figure 8 for the parameters dealt with already in Figures1, 3, 4, 5 and 7. The result is satisfactory. Up to 80% conversion the dormant chains contain more than 90% of the consumed monomer if r is kept smaller than 1%.

Comparison with Experiment. So far, we have theoretically confirmed that living radical polymerizations based on the reversible cleavage (eqs 1 and 2) which are slow because of unfavorably small equilibrium constants can be appreciably accelerated by additional initiation. The living character of the resulting polymer and the control of the molecular weight distribution are not largely deteriorated if the external initiation rate is kept below 1% of the initial rate of the cleavage (eq 1). The beneficial acceleration is not directly due to the formation of additional growing chains but to the locking of the radical concentrations [R] at higher and [Y] at smaller values than they would attain otherwise. A 10-fold decrease of the conversion time seems often achievable. However, extended simulations for many kinetic parameters indicate that this is probably the uppermost limit if sufficient control shall be reached. For instance, external radical generation rates of 20% of the internal rate lead to an even faster monomer consumption. However, one the finds conversion independent average degrees of polymerization and polydispersities although some livingness is retained. The process becomes uncontrolled.

To compare the theoretical results with experiment, we analyze data of Fukuda et al. for styrene polymerizations mediated by TEMPO at 114 °C.[11] About 20% monomer conversion required a time of 4 h when 48 mM 2,2,6,6-tetramethyl-1-polystyroxypiperidine (PS−TEMPO) was used without additional initiator, whereas 49% conversion were obtained in the same time when 4 mM *tert*-butyl hydroperoxide was added. The temperature dependence of the cleavage (activation) rate constant of PS−TEMPO[26] gives $k_d = 5.5 \times 10^{-4}$ s^{-1} at 114 °C. The cross-reaction eactivation rate constant is $k_c = 7.6 \times 10^7$ M^{-1} s^{-1} at 125 °C, and it should be nearly temperature independent.[27] These parameters provide the equilibrium constant for the cleavage of PS−TEMPO, $K = 7.8 \times 10^{-12}$ M at 114 °C, while $K = 2.1 \times 10^{-11}$ M has been measured at 125 °C.[26] Using $k_p = 1740$ M^{-1} s^{-1} from the IUPAC evaluation[28] and adopting $k_t = 5 \times 10^8$ M^{-1} s^{-1} for the relatively short chain radicals, we see that eq 23 leads to 9.3% conversion after 4 h at 114 °C if PS−TEMPO were the only radical source. In the absence of *tert*-butyl hydroperoxide the conversion is considerably larger. This is due to the styrene autoinitiation[26] which provides an additional initiation with the rate $R_i = 5 \times 10^{-8}$ M s^{-1} at 114 °C.[29] Hence, one has $r = R_i/k_d[I]_0 = 0.0019$, and this value is well compatible both with the faster conversion (Figure 4), a controlled process and stationary radical concentrations.[26] For 4 mM *tert*-butyl hydroperoxide, Fukuda's conversions[11] lead to an estimated $r = 0.011$, still compatible with a controlled process. For 6 mM *tert*-butyl hydroperoxide, that is $r = 0.016$, deviations from the ideal behavior were observed.[11] This agrees with the theoretical findings that the ratio of the external to the internal radical generation rate should not exceed $r \approx 0.01$ if one wants to accellerate living radical polymerizations without an appreciable loss of control.[30]

Reduction in the Effects of Disproportionation or a Nonradical Decay. Living radical polymerizations controlled by persistent radicals may severely suffer from the disproportionation reaction between the transient and the persistent radicals

$$R_n^{\bullet} + Y^{\bullet} \xrightarrow{k_{cD}} P_n(-H) + YH \qquad (38)$$

This reaction competes with the cross-coupling (eq 2) and leads to an alkene (macromonomer) and an unreactive compound, for instance to hydroxylamines from nitroxides. The same products are also formed in a direct decay which competes with the cleavage (eq 1)

$$R_n{-}Y \xrightarrow{k_{dD}} P_n(-H) + YH \qquad (39)$$

Quite often, failures of living polymerizations were ascribed to these processes.[6e,7b,31−41]

We have shown earlier that the reactions 38 and 39 cause nearly identical effects for equal fractions $f_D = k_{cD}/(k_c + k_{cD}) = k_{dD}/k_d$.[9] They reduce the achievable monomer conversion and increase the final polydispersity. In particular, the concentration of the dormant chains decreases exponentially as[9,36−38]

$$[I] = [I]_0 e^{-f_D k_d t} \qquad (40)$$

Accordingly, this reduces the regeneration of the propagating radicals, and the polymerization ends approximately at the time $t_D \approx 2/(k_d f_D)^{-1}$. This time may be appreciably smaller that the time needed for substantial conversion even if the fraction f_D of the side reaction is small.[9]

As found above, the additional initiation does not affect equilibrium 10 for not too large relative rates r. Therefore, one finds by an extension of the earlier derivations[9] that eq 40 still holds if there is additional initiation, and that the conversion also ends at the time $t_D \approx 2/(k_d f_D)^{-1}$. However, the polymerization rate is enhanced, and larger conversions are reached before reactions 38 and 39 interfere. The simulations of Figure 9 show the beneficial effects of the rate enhancement on the conversion and on the final degree of polymerization for a relative additional radical generation rate $r = 0.001$, a small fraction of disproportionation $f_D = 0.01$ and the other parameters as used before. For $r = 0.001$ the 90% conversion time is lowered by a factor of

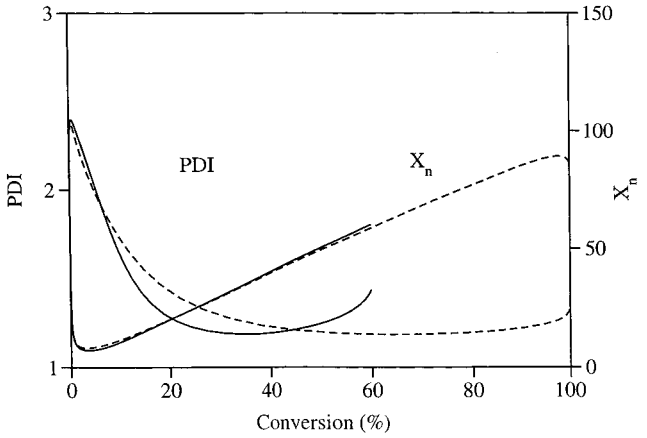

Figure 9. Number average degree of polymerization and polydispersity index as function of conversion for 1% side reaction 38 or 39 ($f_D = 0.01$) in the absence ($r = R_i = 0$, solid lines) and presence ($r = R_i/k_d[I]_0 = 0.001$, broken lines) of additional initiation. Other parameters are as for Figures 1, 3, and 4.

7. Without the additional initiation the maximum conversion is 60%, and the rate enhancement extends this to near completion while the final polydispersity index remains small.

Rate Enhancement by the Removal or the Decay of the Persistent Species

Radical Concentrations and Polymerization Rates. As introduced and widely applied by Georges et al.,[15,42] certain additives enhance the conversion rates of slow living polymerizations because they reduce the retarding build-up of the persistent radicals. Since a reaction between a molecule and a radical always produces another radical the mechanism may involve the transformation of the persistent radical into a transient species which starts a new chain. Müllen et al.[14] showed that unstable triazolinyl radicals which decay thermally to unreactive compounds and initiating radicals offer an advantage over their extremely stable counterparts. Thus, the conversion of styrene was two times larger in the presence of an unstable triazolinyl than for a structurally similar stable species. At 140 °C, the polymerizations took several hours and were living and controlled. However, in the absence of the monomer, the regulating radical decayed at 95 °C in only 15 min. At first sight, the different time scales seem incompatible and call for an explanation.

To analyze the effects of a conversion of the persistent into a transient radical we consider a first-order decay or a pseudo-first-order reaction with an excess substrate

$$Y^\bullet \xrightarrow{k_Y} X + R^\bullet \tag{41}$$

in addition to reactions 1−4 and again search for the upper limit of the rate k_Y which is compatible with a living and controlled process.

Initially, only the regulator and the monomer will be present, and we exclude any further additional initiation. The stoichiometry provides $[I]_0 - [I] = [Y] + [X] = [R] + [P] - [X]$. Obviously, a closed set of kinetic equations now contains three time-dependent variables, and we select [R], [Y], and [X]. The rate equations are

$$d[R]/dt = k_d([I]_0 - [Y] - [X]) - k_c[R][Y] + k_Y[Y] - k_t[R]^2 \tag{42a}$$

$$d[Y]/dt = k_d([I]_0 - [Y] - [X]) - k_Y[Y] - k_c[R][Y] \tag{42b}$$

$$d[X]/dt = k_Y[Y] \tag{42c}$$

In terms of the reduced variables (eq 15) and, in addition, $\xi = [X]/[I]_0$ and $d = k_Y/k_d$, eq 42 becomes

$$\dot{\rho} = 1 - \eta - \xi - a\rho\eta + d\eta - b\rho^2, \tag{43a}$$

$$\dot{\eta} = 1 - \eta - \xi - a\rho\eta - d\eta \tag{43b}$$

$$\dot{\xi} = d\eta \tag{43c}$$

The proper phase space is now three-dimensional (ρ, η, ξ), and the zero isoclines $\eta_1(\rho)$ and $\eta_2(\rho)$ are surfaces which intersect on the line

$$2d\eta = b\rho^2 \tag{44}$$

Figure 10 displays $\eta_1(\rho)$ and $\eta_2(\rho)$ for $\xi = 0$ and for $k_d = k_Y = 3 \times 10^{-3}$ s^{-1}, $k_c = 5 \times 10^7$ M^{-1} s^{-1}, $k_t = 10^8$ M^{-1} s^{-1}, and $[I]_0 = 0.1$ M ($a = 1.67 \times 10^9$, $b = 3.33 \times 10^9$, $d = 1$). These parameters obey the conditions in (5). Also shown is the projection of the trajectory onto the plane (ρ, η, 0). At first, it behaves like the trajectory in Figure 1. After crossing η_1 it also remains confined to the space between the isoclines. In this regime, the equilibrium relation $a\eta\rho = 1$ or (10) holds, and η is given by eq 12. ξ can be obtained by integrating eq 43c but it stays negligibly small. Then, the trajectory reaches the intersecting curve (eq 44) and turns toward the point (0,0,1). For this time regime, a discussion of the isoclines as in ref 7c reveals that equilibrium 10 changes to

$$a\rho\eta = 1 - \xi \tag{45a}$$

or

$$k_c[R][Y] = k_d([I]_0 - [X]) \tag{45b}$$

This is also intuitively expected because the formation of X reduces the concentration of the dormant chains I. Now, eqs 44 and 45 can be combined to express η by ξ, and integration of (43c) yields after the resubstitutions

$$[X] = [I]_0(1 + (t/t_2 - 1)^3) \tag{46}$$

t_2 is given by $t_2 = 3(2[I]_0/K^2k_tk_Y^2)^{1/3}$. At this time, one has $[X] = [I]_0$; that is, R−Y and Y$^\bullet$ are fully converted to X, and the reaction stops. Knowing [X], one finds from (44) and (45) the radical concentrations

$$[R] = \left(\frac{2k_YK[I]_0}{k_t}\right)^{1/3}(1 - t/t_2) \quad \text{and}$$

$$[Y] = \left(\frac{K^2[I]_0{}^2k_t}{k_Y}\right)^{1/3}(1 - t/t_2)^2 \tag{47}$$

Comparison of the expressions for [R] in (47) and (12) reveals that eqs 45−47 start to hold at the approximate time $t_1 = (6k_Y)^{-1}$.

Figure 11 shows a log−log-representation of the concentrations of all species against the time for the parameters used for Figure 10. The decay of Y$^\bullet$ leads to intermediate stationary radical concentrations such as

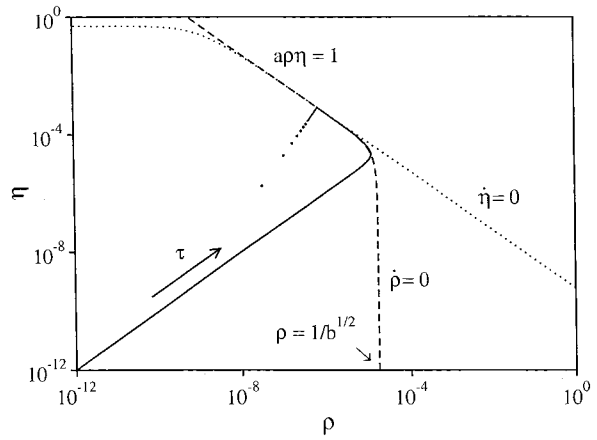

Figure 10. Time evolution of the reduced concentrations ρ and η of the radicals R$^\bullet$ and Y$^\bullet$ and of the isoclines in the projection of the phase space onto the plane (ρ, η, 0) for a decay of the persistent species. Parameters: $a = 1.67 \times 10^9$, $b = 3.33 \times 10^9$, and $d = 1$ ($k_d = k_{dY} = 3 \times 10^{-3}$ s^{-1}, $k_c = 5 \times 10^7$ M^{-1} s^{-1}, $k_t = 10^8$ M^{-1} s^{-1}, $[I]_0 = 0.1$ M).

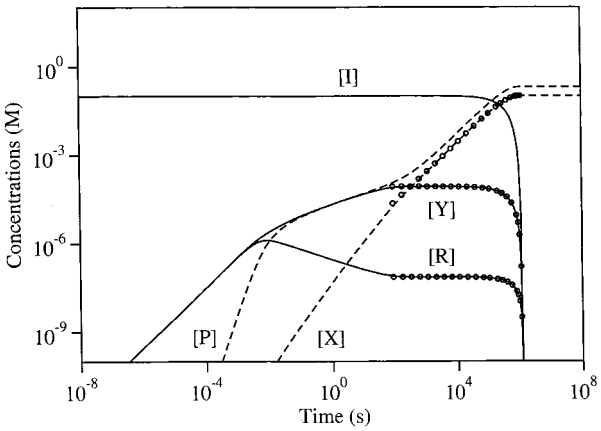

Figure 11. Numerically computed concentrations [R], [Y], [X], and [P] vs time for the parameters given with Figure 10. Lines from numerical calculations and circles are from eqs 46 and 47. The log−log plot serves to enhance the visibility of the different time regimes.

an additional initiation. For the chosen parameters the stationary state is entered at $t_1 = 55$ s which is 6-fold smaller than the natural decay time of Y$^\bullet$, $1/k_Y = 330$ s. It breaks down at the much larger time $t_2 \approx 1.2 \times 10^7$ s = 3300 h. In view of the short natural lifetime of Y$^\bullet$, the long duration of the stationary state is surprising. However, for most of the time Y$^\bullet$ is incorporated in the dormant chains where it does not decay. Hence, Y$^\bullet$ can control a polymerization which lasts much longer than its natural lifetime. Actually, the time fraction in which Y$^\bullet$ is free to decay is approximately given by $[Y]/[I]_0$, and for our parameters this ratio is less than 0.1% of the total time span of the stationary state.

For times $t < t_1$, that is, before the effective onset of the decay of Y$^\bullet$, integration of eq 22 gives the eq 23 for the polymerization index. For the longer time $t_1 < t < t_2$ this becomes

$$\ln\frac{[M]_0}{[M]} = k_p\left(\frac{3K[I]_0}{2^5 k_Y{}^2 k_t}\right)^{1/3} + k_p\left(\frac{2K[I]_0 k_Y}{k_t}\right)^{1/3}\left(t - t_1 - \frac{t^2}{2t_2} + \frac{t_1{}^2}{2t_2}\right) \quad (48)$$

The first term on the right-hand side is very small compared to one if $k_Y \gg (3k_p{}^2K[I]_0/32k_t)^{1/2}$. For our parameters, this holds for $k_Y \gg 10^{-5}$s^{-1} or a natural lifetime of Y$^\bullet$ below 28 h. In realistic cases one will apply persistent radicals with similar or shorter lifetimes, and then the second term dominates. With the further reasonable approximation of conversion only in the stationary state ($t > t_1$), eq 48 reduces to

$$\ln\frac{[M]_0}{[M]} = k_p\left(\frac{2K[I]_0 k_Y}{k_t}\right)^{1/3}\left(t - \frac{t^2}{2t_2}\right) \quad (49)$$

With the earlier given t_2 this leads to the time for 90% monomer conversion

$$t_{90}/t_2 = 1 - \sqrt{1 - \frac{\ln(10)}{3k_p}\left(\frac{2Kk_t{}^2k_Y}{[I]_0{}^2}\right)^{1/3}} \quad (50)$$

The solution (eq 50) exists if the square root is positive, and this requires that the rate constant for the decay of Y$^\bullet$ is smaller than the upper limiting value

$$k_Y < \left(\frac{3k_p}{\ln(10)}\right)^3 \frac{[I]_0{}^2}{2Kk_t{}^2} \quad (51)$$

For our parameters this upper limit is $k_Y = 147$ s^{-1}, and it corresponds to a very fast decay of Y$^\bullet$ in 7 ms. Usually, the decay will be slower. Then one may approximate the square root by its first-order expansion and obtain the simpler result

$$t_{90} = \frac{\ln(10)}{k_p}\left(\frac{k_t}{2K[I]_0 k_Y}\right)^{1/3} \quad (52)$$

Combination of eq 52 with eq 23 gives the ratio of the times for 90% monomer conversion with and without decay of Y$^\bullet$ as

$$\frac{t_{90}(k_Y > 0)}{t_{90}(k_Y = 0)} = \frac{3}{4}\sqrt{\frac{k_p}{\ln(10)}}\left(\frac{2K[I]_0}{k_Y{}^2 k_t}\right)^{1/6} \quad (53)$$

This equation predicts a substantial rate enhancement even for rather small values of k_Y, thas is, for not extremely short lifetimes of Y$^\bullet$. In addition, for a nonzero k_Y, the polymerization index in (50) becomes linear in time as for an additional initiation, and examples are given in Figure 12. From the slopes the decay constant k_Y is obtained if the other rate constants are known.

The rate enhancement is again accompanied by the formation of additional unreactive polymer. For polymerizations in the stationary state one has $[R] \ll [Y] \ll [X]$ (e.g., Figure 11), and the stoichiometry provides $[P] = 2[X]$ for this case. With eq 47 for $t \ll t_{90}$, the expression for t_2 and eqs 12, 23, and 52, one finds the ratio of the unreactive products with and without the decay of the persistent species

$$\frac{[P]_{90}(k_Y > 0)}{[P]_{90}(k_Y = 0)} = \sqrt{\frac{\ln(10)}{k_p}}\left(\frac{k_Y{}^2 k_t}{2K[I]_0}\right)^{1/6} \quad (54)$$

and the comparison with eq 53 leads to

$$\frac{[P]_{90}(k_Y > 0)}{[P]_{90}(k_Y = 0)} = 0.75\frac{t_{90}(k_Y = 0)}{t_{90}(k_Y > 0)} \quad (55)$$

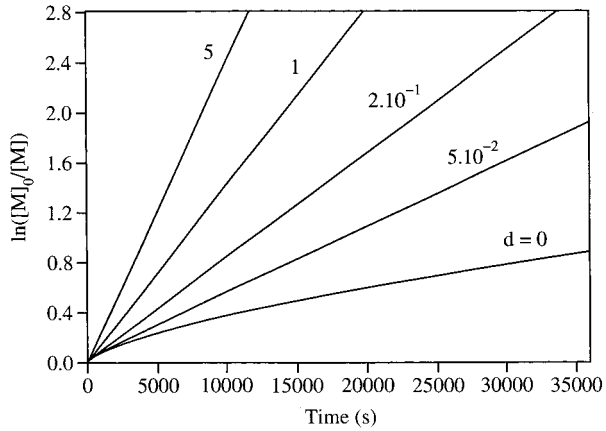

Figure 12. ln([M]$_0$/[M]) vs time, numerically computed for different relative decay rates $d = k_Y/k_d$ of the persistent radical. Other parameters are as for Figure 10, with $k_p = 2000$ M^{-1} s^{-1} and [M]$_0 = 10$ M.

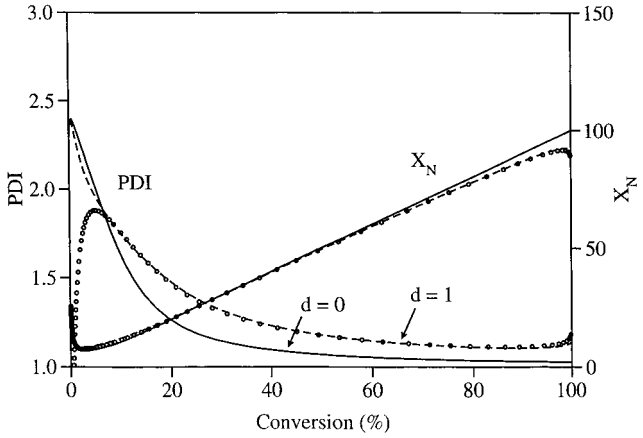

Figure 13. Number average degree of polymerization and polydispersity index as function of conversion with ($d = k_Y/k_d = 1$, $k_Y = 0.003$ s^{-1}) and without ($d = 0$) the decay of the persistent to a transient radical according to numerical calculations (lines) and eqs 57 or 58 (circles). Other parameters are as for Figures 10 and 12.

This relation is formally identical to eq 28. Hence, the rate enhancement and the formation of additional unreactive products by an external initiation and by a decay of the persistent to a transient radical are equally interelated.

Degree of Polymerization, Polydispersity, and Livingness. For a polymerization in the stationary state of the radical concentrations and well before its end at the time t_2 one can approximate the decay product concentration (eq 46) by [X] $= 3[I]_0 t/t_1$. The formation of each X is accompanied by the formation of a polymer chain. Therefore, the zeroth moment becomes

$$m_0 = [I]_0(1 - e^{-k_d t} + 3t/t_1) \tag{56}$$

and one has

$$X_n = \frac{[M]_0 - [M]}{[I]_0(1 - e^{-k_d t} + 3t/t_1)} \tag{57}$$

Equations 33 and 47 lead to the polydispersity index

$$PDI = (1 - e^{-k_d t} + 3t/t_1)\left(1 + k_p\left(\frac{2[I]_0 k_Y}{k_d^2 k_c k_t}\right)^{1/3}\frac{2 - C}{C}\right) + \frac{1}{X_n} \tag{58}$$

For small conversions, this reduces to

$$PDI = (1 - e^{-k_d t} + 3t/t_1)\left(1 + \frac{2}{k_d t}\right) + \frac{1}{X_n} \tag{59}$$

This equation is very similar to (36).

Figure 13 displays X_n and PDI calculated numerically and analytically without ($d = 0$) and with a rather fast decay of the persistent radical ($d = 1$, $k_Y = k_d = 3 \times 10^{-3}$ s^{-1}, and natural lifetime = 330 s) and the other parameters as used before. Even for this fast decay the control remains satisfactory. On the other hand, the time for 90% conversion is reduced by a factor of about 6. The fraction of unreactive products increases by a factor of about 5, but it does not exceed 4% at 90% conversion. Further simulations revealed that even for a natural lifetime of Y$^\bullet$ which is five times shorter than that of the dormant chains ($d = 5$), the monomer fraction in the dormant chains remains above 90% for 80% conversion. Although the given examples refer to the chosen parameters only, this reveals a considerable potential of the application of semipersistent radicals for control as long as they do not decay while bound to the dormant chains. From the arguments given in the previous section it is clear that the rate enhancement by decay is also beneficial to diminish the detrimental effects of the reactions 38 and 39.

Retardation by Initial Persistent Species

Radical Concentrations and Polymerization Rates. In controlled polymerizations the time needed for the bond cleavage (eq 1) of a monomer free precursor R$_0$−Y must be much smaller than the total conversion time. Otherwise, one obtains polymers with large living fractions but little control.[7] For monomers with large propagation constants k_p, this feature has been observed. In this section, we consider the counter-strategy to add persistent species before the reactions.[16−19,22,41] In part, this has also been covered by Fukuda et al.,[13] and the effects of the initial Y$^\bullet$ are easily foreseen.

At first, the transient radicals are simply scavenged by the initial persistent species. Hence, their concentration will be smaller than without the initial excess of Y$^\bullet$. Thus, the monomer conversion rate is lowered and the amount of self-termination is diminished. This improves the control. In an equilibrium of the reactions 1 and 2 the concentration of the transient radicals attains the stationary value [R]$_s = K[I]_0/[Y]_0$, and hence, the polymerization index ln([M]$_0$/[M]) shows a linear time dependence. However, as time proceeds the ever present self-termination of the propagating radicals causes an additional build-up of Y$^\bullet$. When this exceeds the initial concentration [Y]$_0$, the behavior of the system turns to that observed without the initial persistent species.

For a closer examination we consider the basic mechanism (eqs 1−4) and again only cases for which the conditions (eq 5) on the rate constants are fulfilled. The stoichiometry provides [I]$_0$ − [I] = [Y] − [Y]$_0$ = [R] + [P] and gives rise to the closed set of kinetic equations

$$\frac{d[R]}{dt} = k_d([I]_0 + [Y]_0 - [Y]) - k_c[R][Y] - k_t[R]^2 \quad (60a)$$

$$\frac{d[Y]}{dt} = k_d([I]_0 + [Y]_0 - [Y]) - k_c[R][Y] \quad (60b)$$

A comparison with the stoichiometry for $[Y]_0 = 0$, that is, $[I]_0 - [I] = [Y] = [R] + [P]$, suggests that one uses a new time-dependent variable, namely that part of the persistent radical concentration which is provided by the self-termination, $[Y] - [Y]_0$. Consequently, we now use the reduced variable $\tilde{\eta} = [Y] - [Y]_0/[I]_0$, and we denote the initial excess of Y$^\bullet$ by $\eta_0 = [Y]_0/[I]_0$. With the other abbreviations (eq 15), the kinetic equations become

$$\dot{\rho} = 1 - \tilde{\eta} - a\rho(\tilde{\eta} + \eta_0) - b\rho^2 \quad (61a)$$

$$\dot{\tilde{\eta}} = 1 - \tilde{\eta} - a\rho(\tilde{\eta} + \eta_0), \quad (61b)$$

and they are again analyzed in phase space. The zero isoclines $\tilde{\eta}_1(\rho)$, where $\dot{\rho} = 0$, and $\tilde{\eta}_2(\rho)$, where $\dot{\tilde{\eta}} = 0$, are

$$\tilde{\eta}_1(\rho) = \frac{1 - a\rho\eta_0 - b\rho^2}{1 + a\rho} \text{ and } \tilde{\eta}_2(\rho) = \frac{1 - a\rho\eta_0}{1 + a\rho} \quad (62)$$

Figure 14 shows a log−log representation of these isoclines for two excess concentrations $\eta_0 = 10^{-6}$ (0.0001%) and $\eta_0 = 10^{-2}$ (1%) and for the parameters $k_d = 10^{-3}$ s^{-1}, $k_c = 10^7$ M^{-1} s^{-1}, $k_t = 10^8$ M^{-1} s^{-1}, and $[I]_0 = 0.1$ M ($a = 10^9$, $b = 10^{10}$). They intersect the ρ-axis at

$$\rho_1 = (a\eta_0/2b)(\sqrt{1 + 4b/(a\eta_0)^2} - 1) \quad \text{and} \quad \rho_1 = 1/a\eta_0 \quad (63)$$

For $\eta_0 = 10^{-6}$ these intersections are distinct, but they nearly coincide for $\eta_0 \gg \sqrt{b}/a = 10^{-4}$, as it is seen for $\eta_0 = 10^{-2}$. In both cases, they also coincide in a region where the equilibrium relation $a\tilde{\eta}\rho = 1$ holds.

Figure 14 also displays the trajectories for the two excess concentrations. As before, they start along the first diagonal, cross the isocline $\tilde{\eta}_1$ and are confined to the region between $\tilde{\eta}_1$ and $\tilde{\eta}_2$, thereafter. For the small $\eta_0 = 10^{-6}$, the first stage of the time evolution is directly followed by the equilibrium regime $a\tilde{\eta}\rho = 1$, that is, the trajectory is not at all influenced by the initial persistent species. Then eq 12 hold for the concentrations [R] and $[Y] - [Y]_0$. For $\eta_0 = 10^{-2}$, there is an intermediate region of constant ρ. Here, one has from eq 63 $a\eta_0\rho = 1$, and the line $a\tilde{\eta}\rho = 1$ is reached only later. Generally, for $\eta_0 \gg \sqrt{b}/a$ both regimes can be presented by the common relation $a(\tilde{\eta} + \eta_0)\rho = 1$, and this is the usual equilibrium 10.

It is important to note that for a sufficiently large excess of the persistent species $\eta_0 \gg \sqrt{b}/a$ the region of a constant ρ exists, and the equilibrium equation $a\eta_0\rho = 1$ holds even if the equilibrium line $a\tilde{\eta}\rho = 1$ is not reached if $[Y]_0 = 0$. This happens when the rate constants do not obey the conditions in (5), because the equilibrium constant of reactions 1 and 2 is too large. Normally, it leads to fast and uncontrolled polymerizations. Obviously, they can be forced to control by a sufficiently large initial concentration of the persistent species.

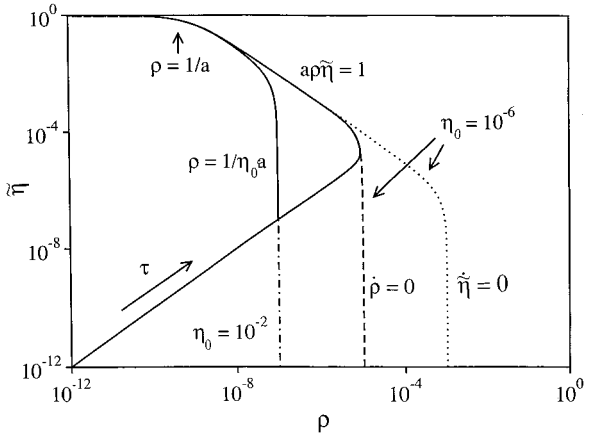

Figure 14. Time evolution of the reduced concentrations ρ and $\tilde{\eta}$ of the radicals R$^\bullet$ and Y$^\bullet$ and isoclines in the phase space for two initial persistent radical concentrations $\eta_0 = 10^{-2}$ and $\eta_0 = 10^{-6}$. Parameters: $a = 10^9$ and $b = 10^{10}$ ($k_d = 3 \times 10^{-3}$ s^{-1}, $k_c = 10^7$ M^{-1} s^{-1}, $k_t = 10^8$ M^{-1} s^{-1}, $[I]_0 = 0.1$ M, $[Y]_0 = 10^{-3}$ M, and $[Y]_0 = 10^{-7}$ M).

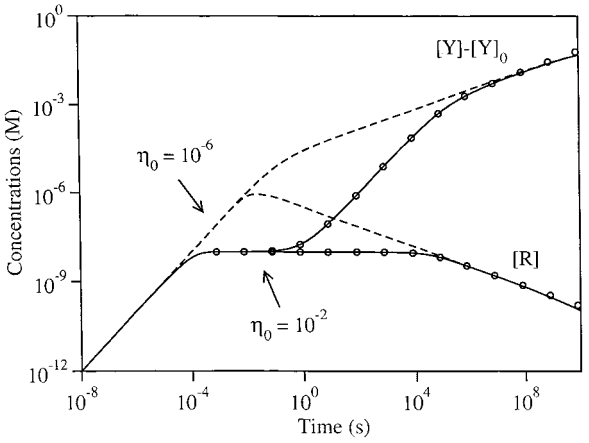

Figure 15. Radical concentrations [R] and $[Y] - [Y]_0$ vs time for the parameters given with Figure 14. Lines from numerical calculations and circles from eq 64 and the equilibrium relation. The log−log plot serves to enhance the visibility of the different time regimes.

Figure 15 shows a log−log representation of the radical concentrations [R] and $[Y] - [Y]_0$ vs time. They were calculated for the same parameters a and b as used for Figure 14. For the small initial concentration $[Y]_0 = 10^{-7}$ M ($\eta_0 = 10^{-6}$) [R] and [Y] develop as for $[Y]_0 = 0$ (cf. Figure 3 for $r = 0$). The larger $[Y]_0 = 10^{-3}$ M leads to a regime where [R] is constant, $[R] = K[I]_0/[Y]_0$. Here, $[Y] - [Y]_0$ first attains the same value as [R]. Then it increases linearly with time while [R] stays constant. This regime is entered at the time $t_1 = 1/k_c[Y]_0$ where $[R] = [Y] - [Y]_0 = k_d[I]_0t_1 = K[I]_0/[Y]_0$. It corresponds to the vertical part of the trajectory in Figure 14. t_1 is in the millisecond region. After the rather long time $t_2 = [Y]_0^3/3K^2[I]_0 2k_t$ eq 12 holds; that is, [R] decreases proportional to $t^{-1/3}$, and $[Y] - [Y]_0$ increases proportional to $t^{1/3}$.

Analytical solutions for the intermediate ($t_1 < t < t_2$) and the final ($t > t_2$) time regimes are also easily derived. Using the relation $\tilde{\eta} = \dot{\rho} + b\rho^2$ which follows from eq 61 and the combined equilibrium $a(\tilde{\eta} + \eta_0)\rho = 1$, one obtains an implicit equation for the time dependence of $\tilde{\eta}$ as for $\eta_0 = 0$.[7] With the appropriate resubstitutions, it provides the approximate solution

$$[Y] = (3k_t K^2 [I]_0^2 (t - t_1) + [Y]_0^3)^{1/3} + K[I]_0/[Y]_0 \quad (64)$$

Apart from the small last term, this equation has been proposed earlier by Fukuda et al.[13] As these authors state, it does not correspond to a simple power law. The expansion of the third root yields the linear increase of [Y] in the intermediate region

$$[Y] = [Y]_0 + \left(K\frac{[I]_0}{[Y]_0}\right)^2 k_t t \quad (65)$$

[R] is then determined by [Y] and the equilibrium relation 10. In Figure 15, the radical concentrations calculated from the preceding analytical equations are presented by circles, and they agree very well with the numerical results.

The rate equation for the monomer (eq 22) is integrated using $[R] = [R]_s = K[I]_0/[Y]_0$ before the time t_2 and eq 13, thereafter. Hence

$$\ln\frac{[M]_0}{[M]} = k_p K\frac{[I]_0}{[Y]_0}t, \quad \text{for } t < t_2, \quad (66a)$$

and

$$\ln\frac{[M]_0}{[M]} = k_p\frac{[Y]_0^2}{3K[I]_0^2 k_t} + \frac{3}{2}k_p\left(\frac{K[I]_0}{3k_t}\right)^{1/3}(t^{2/3} - t_2^{2/3}),$$
$$\text{for } t > t_2 \quad (66b)$$

If $[Y]_0 < (3K[I]_0 k_t/k_p)^{1/2}$, the monomer conversion is governed by the last term of eq 66b. Then, the initial presence of the persistent species has no influence, and the polymerization index varies with time as $t^{2/3}$. On the other hand, 90% conversion is obtained in the stationary state of [R] if $[Y]_0 > (3[\ln(10)]K[I]_0 k_t/k_p)^{1/2}$. For a monomer with a large propagation constant of k_p = 20 000 M^{-1} s^{-1}, and the other parameters $K = 10^{-10}$ s^{-1}, $k_t = 10^8$ M^{-1} s^{-1}, and $[I]_0 = 0.1$ M as before, the first situation is met for $[Y]_0/[I]_0 < 0.004$, that is for 0.4% initial persistent species, and the second for $[Y]_0/[I]_0 >$ 0.006 or for 0.6%. In the latter case, the polymerization index increases linearly with time (eq 66a).

Figure 16 shows polymerization indices calculated with the same parameters as Figures 14 and 15 and, in addition, a rather large propagation constant k_p = 20 000 M^{-1} s^{-1} and several initial concentrations of the persistent species. For $[Y]_0 = 0$, the time for 90% conversion is about 1 h. It increases to about 6.5 h for $[Y]_0 = 2 \times 10^{-3}$ M. As predicted, the time dependence becomes more and more linear with increasing $[Y]_0$. There are deviations of the analytical from the numerical data, due to the fact that the transition between the time regimes does not occur instantaneously as it was assumed to obtain the analytical eq 66b.

According to the previous results, the time dependence of the polymerization index changes from the nonlinear (eq 66b) to the linear behavior (eq 66a) at a critical concentration $[Y]_{0c} \approx (3K[I]_0 k_t/k_p)^{1/2}$. This limit increases with increasing equilibrium constant K and increasing initial regulator concentration $[I]_0$, and it decreases with increasing propagation constant. In fast living polymerizations of acrylates mediated by alkoxyamines with high equilibrium constants, one often improves the control by adding a few percent of the corresponding nitroxide relative to the initiator concentration. For reasonable rate constants and initial concentrations of R_0−Y this percentage is above the required critical value.

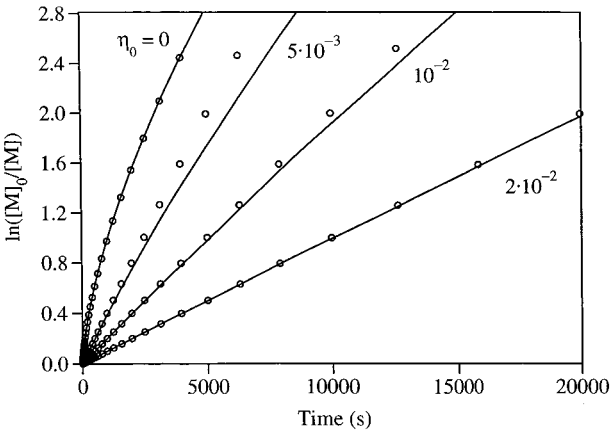

Figure 16. ln($[M]_0/[M]$) vs time for different relative initial concentrations $[Y]_0/[I]_0$ of the persistent radical. Parameters as for Figure 14, k_p = 20 000 M^{-1} s^{-1} and $[M]_0$ = 10 M. Lines are according to numerical calculations, and circles are according to eq 66b.

Recently, Klumperman et al.[43] observed the predicted change of the rate law in polymerizations of methyl methacrylate at 90 °C mediated by a copper complex. Translating the equations for the polymerization index to such ATRP systems, one finds that for large initial concentrations of the Cu(II) complex it is given by an equation first suggested by Matyjaszewski et al.[44]

$$\ln\frac{[M]_0}{[M]} = k_p K\frac{[Cu(I)]_0[I]_0}{[Cu(II)]_0}t \quad (67a)$$

For negligibly small $[Cu(II)]_0$, the polymerization index obeys[7]

$$\ln\frac{[M]_0}{[M]} = \frac{3}{2}k_p\left(\frac{K[Cu(I)]_0[I]_0}{3k_t}\right)^{1/3}t^{2/3} \quad (67b)$$

Here, $[I]_0$ is the initial concentration of the initiating alkyl halide. The transition from the nonlinear to the linear behavior occurs when $[Cu(II)]_0$ exceeds $(3K[Cu(I)]_0[I]_0 k_t/k_p)^{1/2}$, and it was found at a ratio $[Cu(II)]_0/[Cu(I)]_0 \approx 0.1$ or 10%. This is larger than for nitroxide-based systems, but it agrees also with expectations because of the faster ATRP activation step.

Following the earlier procedures, the ratio of the times for 90% monomer conversion with and without an initial excess of the persistent species becomes

$$\frac{t_{90}([Y]_0 > 0)}{t_{90}([Y]_0 = 0)} = \frac{3}{2}[Y]_0(k_p/2\ln(10)K[I]_0 k_t)^{1/2} \quad (68)$$

This ratio is again linearly related to the relative yield of the unreactive products as

$$\frac{[P]_{90}([Y]_0 > 0)}{[P]_{90}([Y]_0 = 0)} = 0.75\,\frac{t_{90}([Y]_0 = 0)}{t_{90}([Y]_0 > 0)} \quad (69)$$

Degree of Polymerization, Polydispersity, and Livingness. In the derivation of the moments one has now to consider the reformation of the initiator I_0 by the coupling of R_0 with the excess $Y^\bullet$. This process competes with the addition of $R_0^\bullet$ to the monomer and leads to a reduction of the effective decay rate of I_0 by

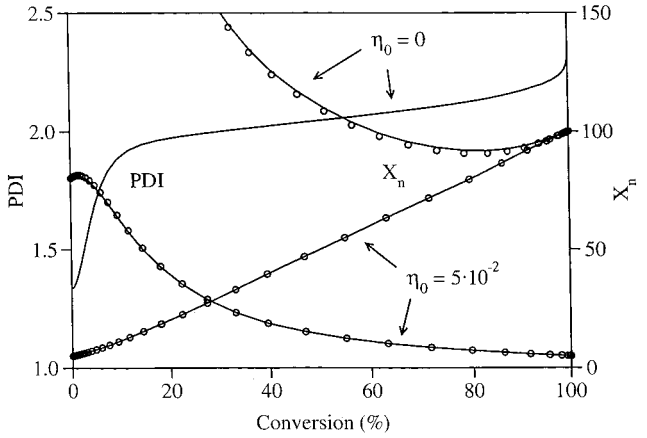

Figure 17. Number average degree of polymerization and polydispersity index as function of conversion for different relative initial concentrations $[Y]_0/[I]_0$ of the persistent radical. Lines are according to numerical calculations, and circles were calculated with eqs 70 and 71. Other parameters are as for Figures 14 and 16.

the probability factor $\beta = k_p[M]_0/(k_p[M]_0 + k_c[Y]_0)$. Hence, the zeroth moment is now given by $m_0 = [I]_0(1 - \exp(-\beta k_d t))$. The other equations of the moments are unchanged. Therefore, X_n becomes

$$X_n = \frac{[M]_0 - [M]}{[I]_0(1 - e^{-\beta k_d t})} \tag{70}$$

If the excess $[Y]_0$ leads to a constant radical concentration $[R]_s = K[I]_0/[Y]_0$ during the whole polymerization, the integration of eq 33 and use of the definition provides the polydispersity index

$$PDI = (1 - e^{-\beta k_d t})\left(1 + \frac{k_p[I]_0}{k_c[Y]_0}\frac{2 - C}{C}\right) + \frac{1}{X_N} \tag{71}$$

For small conversions and sufficiently long times this reduces to eq 36, and the exponential terms must again be dropped if macroinitiators are used.

Figure 17 shows X_n and PDI as functions of conversion for the same parameters as used for Figure 16 and for 0% and 5% initial persistent species. For 0% the rather fast polymerization shows little control, and for 5% the beneficial effects of an initial persistent species are obvious. The much better control is obtained on the expense of a strong retardation of the conversion. For the chosen parameters it amounts to a 150-fold longer 90% conversion time. Further, the initial persistent species increases the livingness but also enhances the deteriorating effects of reactions 38 and 39.

Finally, we note from Figure 17 that in the initial presence of the persistent radical the average degree of polymerization X_n increases with increasing monomer conversion as usual but it starts from a well defined value. In all other cases, it undergoes an initial decrease that is seen, e.g., in Figures 5, 9, and 13. In fact, by use of eqs 66a and 70, one derives easily that for $C \to 0$ and $[Y]_0 \neq 0$ one has initially

$$X_{n,0} = 1 + k_p[M]_0/k_c[Y]_0 \tag{72}$$

This equation may be used to obtain the cross-coupling constant k_c from X_n if the other parameters are known.

Acknowledgment. We thank the Swiss National Foundation for Scientific Research and CSC, Basel, for support, and Prof. T. Fukuda, Kyoto, for an illuminating correspondence.

References and Notes

(1) Solomon, D. H.; Rizzardo, E.; Cacioli, P. U.S. Pat. 4581429, *Chem. Abstr.* **1985**, *102*, 221335q.
(2) Georges, M. K.; Veregin, R. P. N.; Kazmaier, P. M.; Hamer, G. K. *Macromolecules* **1993**, *26*, 2987.
(3) An overview is provided by the articles in Controlled/Living Radical Polymerization (*ACS Symp. Ser.* **2000**, *768*) and the references given therein.
(4) Bachmann, W. E.; Wiselogle, F. Y. *J. Org. Chem.* **1936**, *1*, 354. Perkins, M. J. *J. Chem. Soc.* **1964**, 5932. Fischer, H. *J. Am. Chem. Soc.* **1986**, *108*, 3925. Ruegge, D.; Fischer, H. *Int. J. Chem. Kinet.* **1989**, *21*, 703. Kothe, T.; Martschke, R.; Fischer, H. *J. Chem. Soc., Perkin Trans. 2* **1998**, 503. Wagner, P. J.; Thomas, M. J.; Puchalski, A. E. *J. Am. Chem. Soc.* **1986**, *108*, 7739. Walling, C. *J. Am. Chem. Soc.* **1988**, *110*, 6846. Daikh, E.; Finke, R. G. *J. Am. Chem. Soc.* **1992**, *114*, 2939. MacFaul, P. A.; Arens, I. W. C. E.; Ingold, K. U.; Wayner, D. D. M. *J. Chem. Soc., Perkin Trans. 2* **1997**, 135. Bravo, A.; Bjorsvik, H.-R.; Fontana, F.; Liguori, L.; Minisci, F. *J. Org. Chem.* **1997**, *62*, 3849. Karatekin, E.; O'Shaughnessy, B.; Turro, N. J. *J. Chem. Phys.* **1998**, *108*, 9577. Studer, A. *Chem.—Eur. J.* **2000**, *7*, 1159. Fischer, H. *Chem. Rev.*, submitted for publication, and references therein.
(5) Otsu, T.; Yoshida, M. *Makromol. Chem. Rapid Commun.* **1982**, *3*, 127. Otsu, T.; Yoshida, M. *Makromol. Chem. Rapid Commun.* **1982**, *3*, 133. Otsu, T.; Matsunaga, T.; Kuriyama, A.; Yoshioka, M. *Eur. Polym. J.* **1989**, *25*, 643 and references therein.
(6) (a) Johnson, C. H.; Moad, G.; Solomon, D. H.; Spurling, T. H. Vearing, D. J. *Aust. J. Chem.* **1990**, *43*, 1215. (b) Wayland, B. B.; Pozmik, G.; Mukerjee, S. L. *J. Am. Chem. Soc.* **1994**, *116*, 7943. (c) Wang, J.-S.; Matyjaszewski, K. *J. Am. Chem. Soc.* **1995**, *117*, 5614. Greszta, D., Matyjaszewski, K. *Macromolecules* **1996**, *29*, 7661. (d) Percec, V.; Barboiu, B. *Macromolecules* **1995**, *28*, 7970. (e) Fukuda, T.; Terauchi, T.; Goto, A.; Ohno, K., Tsujii, YS.; Miyamoto, T.; Kobatake, S.; Yamada, B. *Macromolecules* **1996**, *29*, 6393. (f) He, J.; Zhang, H.; Chen, J.; Yang, Y. *Macromolecules* **1997**, *30*, 8010.
(7) (a) Fischer, H. *Macromolecules*, **1997**, *30*, 5666. (b) Fischer, H. *J. Pol. Sci. A*, **1999**, *37*, 1885. (c) Souaille M.; Fischer H. *Macromolecules*, **2000**, *33*, 7378.
(8) Ohno, K.; Tsujii, Y.; Miyamoto, T.; Fukuda, T.; Goto, M.; Kobayashi, K.; Akaike, T. *Macromolecules*, **1998**, *31*, 1064.
(9) Souaille M.; Fischer H. *Macromolecules* **2001**, *34*, 2830.
(10) Greszta, D.; Matyjaszewski, K. *J. Polym. Sci. A* **1997**, *35*, 1857.
(11) Goto, A.; Fukuda, T. *Macromolecules* **1997**, *30*, 4272.
(12) Fukuda, T.; Goto, A. *ACS Symp. Ser.* **2000**, *768*, 27 and references therein.
(13) Fukuda, T.; Goto, A.; Ohno, K. *Macromol. Rapid Commun.* **2000**, *21*, 151.
(14) Klapper, M.; Brand, T.; Steenbock, M.; Müllen, K. *ACS Symp. Ser.* **2000**, *768*, 152 and references therein.
(15) Georges, M. K.; Veregin, R. P. N.; Kazmaier, P. M.; Hamer, G. K.; Saban, M. D. *Macromolecules* **1994**, *27*, 7228.
(16) Benoit, D.; Chaplinski, V.; Braslau, R.; Hawker, C. J. *J. Am. Chem. Soc.* **1999**, *121*, 3904. Benoit, D.; Hawker, C. J.; Huang, E. E.; Lin, Z.; Russell, T. P. *Macromolecules* **2000**, *33*, 1505. Benoit, D.; Harth, E.; Helms, B.; Vestberg, R.; Rodlert, M.; Hawker, C. J. *ACS Symp. Ser.* **2000**, *768*, 122.
(17) Benoit, D.; Grimaldi, S.; Robin, S.; Finet, J.-P.; Tordo, P.; Gnanou, Y. *J. Am. Chem. Soc.* **2000**, *122*, 5929.
(18) Lacroix-Desmazes, P.; Lutz, J.-F.; Boutevin, B. *Macromol. Chem. Phys.* **2000**, *21*, 662.
(19) Bon, A. F.; Bosveld, M.; Klumperman, B.; German, A. L. *Macromolecules* **1997**, *30*, 324.
(20) As in earlier work, we denote the rate constant for the self-termination by k_t instead of $2k_t$ to avoid an overcrowding of the theoretical equations by the numerical factor 2.
(21) Le Mercier, C.; Lutz, J.-F.; Marque, S.; Le Moigne, F.; Tordo, P.; Lacroix-Desmazes, P.; Boutevin, B.; Couturier, J.-L.; Guerret, O.; Martschke, R.; Sobek, J.; Fischer, H. *ACS Symp. Ser* **2000**, *768*, 108 and references therein.
(22) Lutz, J.-F.; Lacroix-Desmazes, P.; Boutevin, B. *Macromol. Rapid Commun.* **2001**, *22*, 189.

(23) Chambard, G.; Klumpermann, B. *ACS Symp. Ser.* **2000**, *768*, 197.
(24) Young, R. J.; Lovell, P. A. *Introduction to Polymers*, 2nd ed.; Chapman & Hall: London, 1991. Elias, H.-G. *Macromolecules*, 2nd ed.; Plenum: New York, 1984.
(25) Fukuda, T.; Goto, A. *Macromol. Rapid Commun.* **1997**, *18*, 683.
(26) Fukuda, T.; Goto, A.; Ohno, K.; Tsujii, Y. *ACS Symp. Ser.* **1998**, *685*, 180 and references therein.
(27) Sobek, J.; Martschke, R.; Fischer, H. *J. Am. Chem. Soc.* **2001**, *123*, 2849 and references therein.
(28) Buback, M.; Gilbert, R. G.; Hutchinson, R. A.; Klumperman, B.; Kuchta, F.-D.; Manders, B. G.; O'Driscoll, K. F.; Russell, G. T.; Schweer, J. *Macromol. Chem. Phys.* **1995**, *196*, 3267.
(29) Hui, A. W.; Hamielic, A. E. *J. Appl. Polym. Sci.* **1972**, *16*, 749.
(30) For related simulations, see also: He, J.; Chen, J.; Li, L.; Pan, J.; Li, C.; Cao, J.; Tao, Y.; Hua, F.; Yang, Y.; McKee, G. E.; Brinkmann, S. *Polymer* **2000**, *41*, 4573. He, J.; Li, L.; Yang, Y. *Macromol. Theory Simul.* **2000**, *9*, 479.
(31) Moad, G.; Anderson, A. G.; Ercole, F.; Johnson, C. H. J.; Krstina, J.; Moad, C. L.; Rizzardo, E.; Spurling, T. H.; Thang, S. H. *ACS Symp. Ser.* **1998**, *685*, 332.
(32) He, J.; Li, L.; Yang, Y.; *Macromolecules* **2000**, *33*, 2286.
(33) Li, I.; Howell, B. A.; Matyjaszewski, K.; Shigemoto, T.; Smith, P. B.; Priddy, D. B. *Macromolecules* **1995**, *28*, 6692.
(34) Skene, W. G.; Scaiano, J. C.; Yap, G. P. A. *Macromolecules* **2000**, *33*, 3536. Skene, W. G.; Scaiano, J. C.; Listigovers, N. A.; Kazmaier, P. M.; Georges, M. K. *Macromolecules* **2000**, *33*, 5065 and references therein.
(35) Moffat, K. A.; Hamer, G. K.; Georges, M. K. *Macromolecules* **1999**, *32*, 1004.
(36) Ohno, K.; Tsujii, Y.; Fukuda, T. *Macromolecules* **1997**, *30*, 2503.
(37) Goto, A.; Terauchi, T.; Fukuda, T.; Miyamoto, T. *Macromol. Rapid Commun.* **1997**, *18*, 673.
(38) Goto, A.; Fukuda, T. *Macromolecules* **1999**, *32*, 618.
(39) Bon, S. A. F.; Chambard, G.; German, A. L. *Macromolecules* **1999**, *32*, 8269.
(40) Chong, B. Y. K.; Ercole, F.; Moad, G.; Rizzardo, E.; Thang, S. H.; Anderson, A. G. *Macromolecules* **1999**, *32*, 6895.
(41) (a) Engel, P. S.; Duan, S.; Arhancet, G. B. *J. Org. Chem.* **1997**, *62*, 3537. (b) Fischer, A.; Brembilla, A.; Lochon, P. *Macromolecules* **1999**, *32*, 6069.
(42) Saban, M. D.; Georges, M. K.; Veregin, R. P. N.; Hamer, G. K.; Kazmaier, P. M. *Macromolecules* **1995**, *28*, 7032. Veregin, R. P. N.; Odell, P. G.; Michalak, L. M.; Georges, M. K. *Macromolecules* **1996**, *29*, 2746. Odell, P. G.; Veregin, R. P. N.; Michalak, L. M.; Georges, M. K. *Macromolecules* **1997**, *30*, 2232. Georges, M. K.; Hamer, G. K.; Listigovers, N. A. *Macromolecules* **1998**, *31*, 9087. MacLeod, P. J.; Veregin, R. P. N.; Odell, P. G.; Georges, M. K. *Macromolecules* **1998**, *31*, 530. Moffat, K. A.; Hamer, G. K.; Georges, M. K. *Macromolecules* **1999**, *32*, 1004 and references therein.
(43) Zhang, H.; Klumperman, B.; Ming, W.; Fischer, H.; van der Linde, R. *Macromolecules*, submitted for publication.
(44) Matyjaszewski, K.; Patten, T. E.; Xia, J. *J. Am. Chem. Soc.* **1997**, *119*, 674.

MA010880H